THE JOURNAL OF PHYSICAL CHEMISTRY A

Article

pubs.acs.org/JPCA

Molecular Dynamics of Methanol Monocation (CH_3OH^+) in Strong Laser Fields

Bishnu Thapa and H. Bernhard Schlegel*

Department of Chemistry, Wayne State University, Detroit, Michigan 48202, United States

Supporting Information

ABSTRACT: Experimental studies by Yamanouchi and co-workers indicate that an intense 40 fs 800 nm laser pulse can cause CH_3OH^+ to isomerizes during the pulse. The potential energy surfaces of methanol neutral, monocation, and singlet and triplet dication were explored using the CBS-APNO, CBS-QB3, CAM-B3LYP, and B3LYP levels of theory. Ab initio classical trajectories were calculated in the presence of a 2.9×10^{14} W/cm^2 800 nm laser field for methanol monocation on the ground state potential energy surface using the CAM-B3LYP/6-31G(d,p) level of theory. With only zero point energy, CH_3OH^+ gained less than 15 kcal/mol from the 40 fs laser pulse, which was not enough to overcome any of the barriers for isomerization or fragmentation. To simulate extra energy deposited during the ionization process, 75, 100, and 125 kcal/mol of vibrational energy was added to the initial structures. After 400 fs, the distribution of product was CH_2OH^+ + H (79−81%), $HCOH^+$ + H_2 (9−13%), $CH_2OH_2^+$ (1−3%), CH_3^+ + OH (1−3%), and CH_2^+ + H_2O (<0.5%). The estimated kinetic energy releases are in accord with experimental findings. Experimental results using a probe pulse to ionize CH_3OH^+ to the dication showed substantial fraction C−O dissociation in both CH_3OH^+ and $CH_2OH_2^+$ after the pulse. Because very few $CH_2OH_2^+ \rightarrow CH_2^+ + H_2O$ trajectories were seen in the simulation, the calculations suggest that some of the processes observed experimentally must occur on excited state surfaces or may be due to coupled nuclear-electron dynamics during the pump pulse.

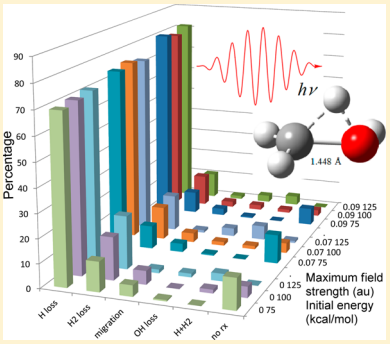

INTRODUCTION

In a series of recent papers, Yamanouchi and co-workers have examined the fragmentation of methanol by intense 800 nm laser pulses, with an aim to understanding the behavior of methanol mono- and dications in strong laser fields.[1−8] They measured the kinetic energy release for H_2^+ and H_3^+ ejected from the mono-, di-, and trications of methanol.[1] By comparing the yield of HD^+ and D_2^+ from CD_3OH, they were able to estimate the H/D exchange rate in the ion.[1] Coincidence momentum imaging was used to identify the hydrogen ejection processes for the dication, $CH_3OH^{2+} \rightarrow CH_{3-n}OH^+ + H_n^+$, and angular distribution patterns were used to estimate lifetimes.[2,3] The three-body Coulomb explosion of the trication, $CH_3OH^{3+} \rightarrow HCO^+ + H^+ + H_2^+$ was found to occur in a stepwise manner, with either H^+ or H_2^+ ejected first.[4] Coincidence momentum imaging revealed that hydrogen migration occurred in the dication within the laser pulse.[5] For pulse lengths of 7, 21, and 60 fs, the relative yields of $CH_3OH^{2+} \rightarrow CH_3^+ + OH^+$ and $CH_3OH^{2+} \rightarrow CH_2OH_2^{2+} \rightarrow CH_2^+ + H_2O^+$ were 1:0.13, 1:0.17, and 1:0.50.[6] A pump−probe coincidence momentum imaging method was used to study ultrafast hydrogen migration.[7,8] The 38 fs 800 nm pump pulse produced methanol monocation, and a probe pulse delayed by 100−800 fs was used to generate the dication whose fragments were detected by coincident momentum imaging. With the help of the ground state potential energy surface of methanol monocation, the results were interpreted in terms of ultrafast hydrogen migration driven by the laser pulse, and slower migration and fragmentation occurring after the pulse.[7,8] As a first step in studying the isomerization and fragmentation of methanol by intense laser pulses, we have used ab initio classical trajectory calculations to investigate the dynamics of methanol monocation on the ground state potential energy surface in the presence of a strong laser field.

The potential energy surface for neutral methanol is well-known experimentally and has been the subject of numerous computational studies (for early work see refs 9 and 10; for recent MRCI calculations, see ref 11). In contrast, the potential energy surfaces for the mono- and dications of methanol have some unexpected features. Calculations of the monocation potential surface by Bouma, Nobes, and Radom[12] showed that the lowest energy structure is $H_2COH_2^+$ and not CH_3OH^+; this was quickly confirmed experimentally.[13,14] Pople, Radom, and co-workers[15] mapped out the CH_3OH^+ potential energy surface at the G2[16] level of theory and found very good agreement with available experimental data. Wiest[17] demonstrated that B3LYP calculations of the CH_3OH^+ surface were in good agreement with the G2 calculations. More detailed calculations by Radom and co-workers refined the energy difference between is $H_2COH_2^+$ and CH_3OH^+ [18] and showed the latter had an eclipsed conformation.[19] The fragmentation of doubly ionized methanol has been studied experimentally by

Received: October 10, 2013
Revised: January 22, 2014
Published: February 18, 2014

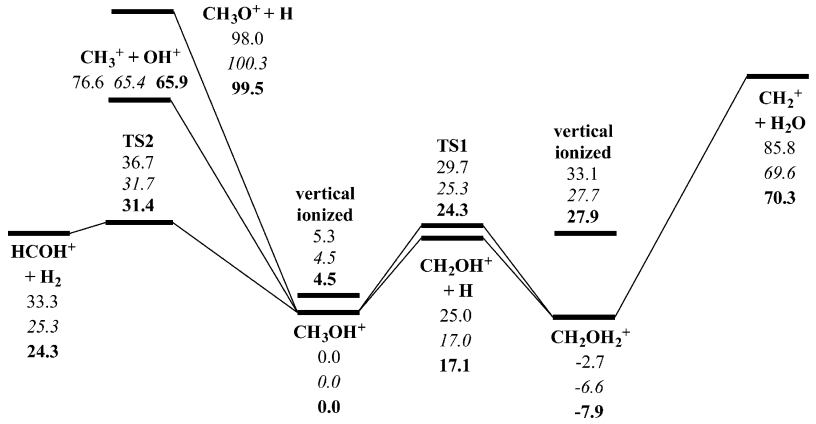

Figure 1. Relative enthalpies at 0 K in kcal/mol for CH_3OH^+ calculated at the CAM-B3LYP/6-31G(d,p), CBS-QB3 (italics), and CBS-APNO (bold) levels of theory. The CH_3OH^+ minimum is 239.0, 251.8, and 251.9 kcal/mol above CH_3OH at the CAM-B3LYP/6-31G(d,p), CBS-QB3, and CBS-APNO levels of theory, respectively.

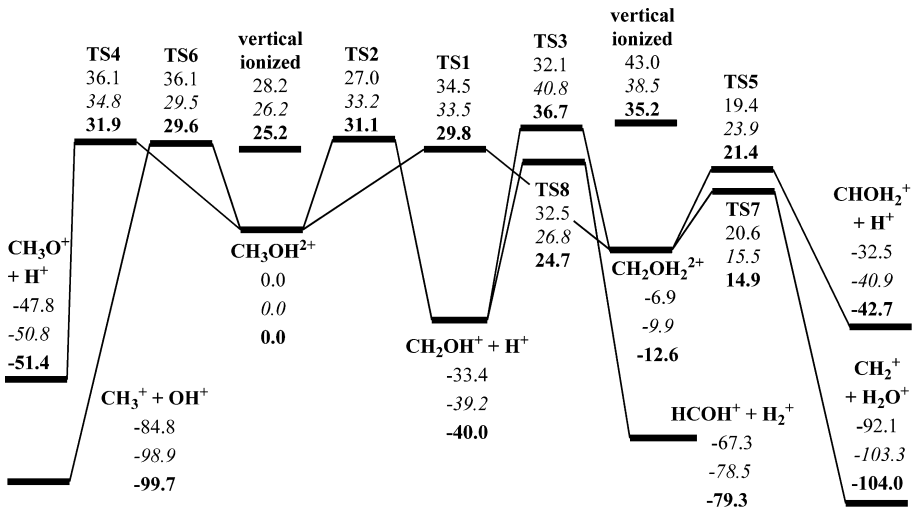

Figure 2. Relative enthalpies at 0 K in kcal/mol for triplet CH_3OH^{2+} calculated at the CAM-B3LYP/6-31G(d,p), CBS-QB3 (italics), and CBS-APNO (bold) levels of theory. The triplet CH_3OH^{2+} minimum is 697.8, 716.5, and 717.1 kcal/mol above CH_3OH at the CAM-B3LYP/6-31G(d,p), CBS-QB3, and CBS-APNO levels of theory, respectively.

Eland and co-workers using photoionization and photoelectron-photoion-photoion-coincidence (PEPIPICO) detection.[20,21] Radom and co-workers explored the potential energy surface for the singlet dication and found $H_2COH_2^{2+}$ to be much more stable than CH_3OH^{2+}.[22,23]

In prior work, we have used Born−Oppenheimer molecular dynamics to explore the dissociation of energized mono- and dications under field-free conditions and within a laser pulse.[24−28] Laser fields in the optical range were found to enhance the decomposition of H_2NCH^{2+}.[26] For oriented $ClCHO^+$, mid-IR laser pulses promoted reaction channels that were energetically and entropically disfavored.[28] The aim of this initial study is to explore the effect of an intense 800 nm laser pulse on the isomerization and fragmentation of methanol cation on the ground state potential energy surface. Further studies can address dynamics on excited state surfaces and the possibility of coupled nuclear-electron dynamics during the pump pulse.

METHODS

Calculations were carried out with the development version of the Gaussian series of programs.[29] Geometries were fully optimized; vibrational frequencies were computed to obtain zero point energies and to confirm that the structures were either minima or transition states. Reaction enthalpies at 0 K were calculated with the CBS-APNO,[30] CBS-QB3,[31] and G4[32] compound methods, and with second-order Møller−Plesset perturbation theory and density functional theory using the B3LYP[33−37] and CAM-B3LYP[38] functionals with the 6-31G(d,p) and 6-311++(d,p) basis sets. For some of the CBS-APNO calculations of the dication transition states, zero point energy was calculated using the QCISD optimized geometry.

The strong electric field of an intense laser pulse will distort the electron density of a molecule and thereby affect its dynamics. One way to test whether a given level of theory adequately models the response of the density to the electric field is to examine the dipole moment. A plot of the dipole moment of CH_3OH^+ as a function of a static field directed along the C−O bond is shown in Figure S1 of the Supporting Information. Compared to CCSD(T), Hartree−Fock and MP2 show the wrong behavior. DFT methods like B3LYP and CAM-B3LYP (as well as related long-range corrected functionals, not shown) agree quite well with the CCSD(T) curve.

dx.doi.org/10.1021/jp410091b | J. Phys. Chem. A 2014, 118, 1769−1776

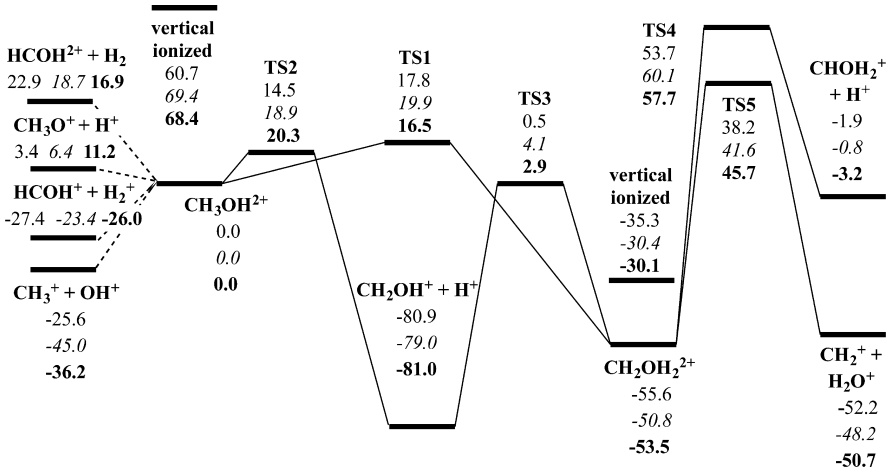

Figure 3. Relative enthalpies at 0 K in kcal/mol for singlet CH_3OH^{2+} calculated at the CAM-B3LYP/6-31G(d,p), CBS-QB3 (italics), and CBS-APNO (bold) levels of theory. The singlet CH_3OH^{2+} minimum is 658.0, 661.4, and 663.8 kcal/mol above CH_3OH at the CAM-B3LYP/6-31G(d,p), CBS-QB3, and CBS-APNO levels of theory, respectively.

Classical trajectories were computed on the ground state potential energy surface using our recently developed Hessian-based predictor-corrector algorithm for simulating molecular dynamics in a laser field.[39] In this method the surface is approximated by a distance weighted interpolant (DWI) using the first and second derivatives of the energy. The first derivatives of the gradient with respect to the electric field are also included in the predictor and the corrector steps. The velocity Verlet method with δt = 0.0025 fs is used to integrate both the predictor and corrector steps on the DWI surface. An overall step size of Δt = 0.25 fs is employed and the Hessian is updated[40,41] for 20 steps before being recalculated analytically. A Ti:sapphire laser pulse was modeled by a time varying electric field with a wavelength of 800 nm. The pulse length was 15 cycles (40 fs) with either a trapezoidal envelope (increasing linearly for the first cycle and decreasing linearly for the last cycle) or a cosine squared envelope. The maximum field strengths were 0.09 au (2.9×10^{14} W/cm^2) and 0.07 au (0.88×10^{14} W/cm^2). The direction of the laser field was chosen randomly and the starting structures had no rotational energy. Zero point energy and any additional vibrational energy were added to the initial structure using orthant sampling of the momentum.[42]

RESULTS AND DISCUSSION

Structures and Energetics. The energetics for the fragmentation of methanol neutral, monocation and dication are summarized in Figures 1−3 and in Tables S1−S4 of the Supporting Information. Because the trajectory calculations focus on the dynamics of methanol monocation in strong laser fields, it is appropriate to use the potential energy surface of the monocation to examine the accuracy for the different computational models. Table S2 (Supporting Information) shows that the CBS-APNO, CBS-QB3, and G4 levels of theory agree very well with each other and published high level calculations,[11,15,18,19,23] and therefore these will be used as reference values. Hartree−Fock calculations are not expected to be adequate because many of the reactions are bond dissociations. MP2 calculations generally underestimate the reaction energies and B3LYP calculations overestimate the reaction energies. The CAM-B3LYP data are in somewhat better agreement with the high level calculations. The CAM-B3LYP functional has the added advantage of better long-range behavior, which may be important for treating the distortion of the electron density by the strong laser fields. With the exception of reactions involving C−O dissociation, increasing the basis set from 6-31G(d,p) to 6-311++G(d,p) had only a modest effect. For the molecular dynamics calculations in strong laser fields, we have chosen CAM-B3LYP/6-31G(d,p) as an appropriate compromise between accuracy and affordability.

For neutral methanol, all of the pathways are strongly endothermic (Table S1, Supporting Information). The O−H bond has the highest dissociation energy (104 kcal/mol at the CBS-APNO level of theory), followed by the C−H bond (94 kcal/mol) and the C−O bond (90 kcal/mol). The 1,2 hydrogen shift to form the CH_2OH_2 ylide is also strongly disfavored (82 kcal/mol). The barrier for the reverse reaction is very small (2 kcal/mol), indicating that neutral CH_2OH_2 is unstable, in contrast to the ylide mono- and dications (see below). The loss of H_2 to give hydroxycarbene has a reaction energy of 77 kcal/mol. The barrier for hydroxycarbene insertion into H_2 (5.6 kcal/mol) is similar to fluorocarbene insertion into H_2[43] (4.6 kcal/mol at CBS-QB3).

Key structures for the CH_3OH^+ potential energy surface are collected in Figure 4. The methanol monocation prefers the eclipsed conformation over staggered at the highest levels of theory.[19] The rotation barrier (1 kcal/mol) is similar to the neutral form. Although there are only high energy dissociation pathways on the neutral methanol potential energy surface, the monocation surface has three low energy channels (Figure 1 and Table S2, Supporting Information). Breaking a C−H bond leads to CH_2OH^+ (17 kcal/mol at CBS-APNO), which has a C−O double bond and can viewed as protonated formaldehyde. The 1,2 hydrogen shift reaction has a barrier of 24 kcal/mol and leads to an ylide cation, $CH_2OH_2^+$, that is 8 kcal/mol more stable than CH_3OH^+. Although the neutral ylide has the H_2O group perpendicular to CH_2, the monocation is nearly planar with the H_2O and CH_2 groups slightly pyramidal in opposite directions. Methanol monocation can also lose H_2 with a barrier of 31 kcal/mol to yield $HCOH^+$ (24 kcal/mol). The dissociation energies of the O−H and C−O bonds in CH_3OH^+ (100 and 66 kcal/mol) and the C−O bond in $CH_2OH_2^+$ (78 kcal/mol) remain high.

dx.doi.org/10.1021/jp410091b | J. Phys. Chem. A 2014, 118, 1769−1776

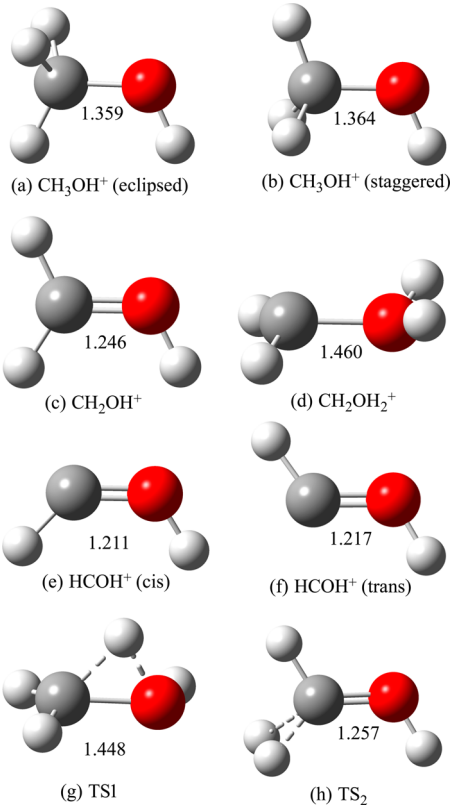

Figure 4. Selected structures on the methanol monocation potential energy surface (bond lengths in Å).

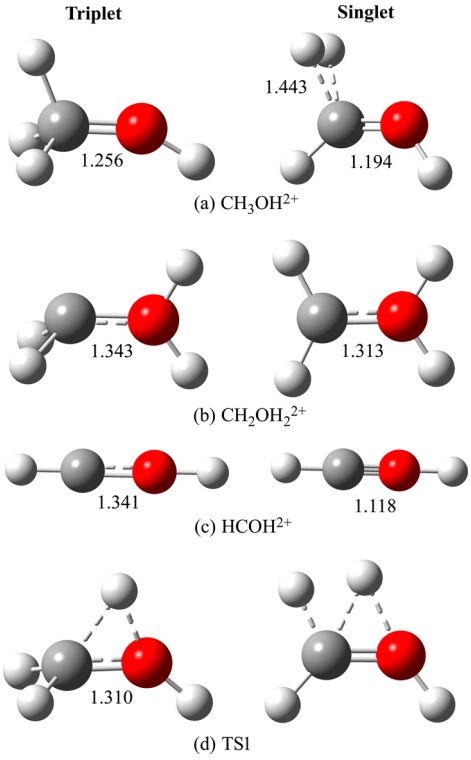

Figure 5. Selected structures of methanol dication on the triplet (left) and singlet (right) potential energy surfaces (bond lengths in Å).

A second ionization of methanol can yield either a singlet or triplet dication (Figures 2 and 3 and Tables S3 and S4, Supporting Information). Selected structures are compared in Figure 5. The geometry of triplet CH_3OH^{2+} is similar to neutral methanol but with a larger HOC angle. Although the open shell singlet CH_3OH^{2+} would be expected to have an analogous structure, all attempts to optimize the geometry lead to a much lower energy $^1A'$ structure, H_2−$HCOH^{2+}$, with two long C−H bonds and a short H−H bond (53 kcal/mol below triplet CH_3OH^{2+} at CBS-APNO). A 1,2 hydrogen shift in CH_3OH^{2+} leads to the ylide dication, $CH_2OH_2^{2+}$. Triplet $CH_2OH_2^{2+}$ resembles the neutral ylide (H_2O group perpendicular to CH_2) and is 13 kcal/mol below CH_3OH^{2+} with a barrier of 30 kcal/mol. The singlet $CH_2OH_2^{2+}$ is planar and can be described as doubly protonated formaldehyde, which is isoelectronic with ethylene. The barrier for its formation from CH_3OH^{2+} is only 17 kcal/mol, and the ylide is 54 kcal/mol more stable than singlet CH_3OH^{2+}. The lowest dissociation channels of the dication surfaces lead to two monocations and have barriers arising from a competition between the increasing energy as bonds are stretched and decreasing Coulomb repulsion as the ions separate. On the triplet surface, the barriers for $CH_3OH^{2+} \rightarrow CH_2OH^+ + H^+$, $CH_3O^+ + H^+$, and $CH_3^+ + OH^+$ are 31, 32, and 30 kcal/mol, respectively, at the CBS-APNO level, and the enthalpies of reaction are −40, −51, and −100 kcal/mol, respectively. The barrier and enthalpy of reaction for singlet $CH_3OH^{2+} \rightarrow CH_2OH^+ + H^+$ are considerably lower (+20 and −81 kcal/mol) because of the greater stability of singlet CH_2OH^+. Because the lowest singlet state of CH_3OH^{2+} is $^1A'$, O−H and C−O dissociation to form $^3\Sigma$ or $^1\Delta$ OH^+ and CH_3O^+ requires a crossing to a different state. Because singlet CH_3OH^{2+} has two long C−H bonds and a short H−H bond, it can dissociate easily to $HCOH^{2+} + H_2$ (17 kcal/mol); crossing to a lower energy surface leads to $HCOH^+ + H_2^+$ (−26 kcal/mol). Formation of H_2^+ is more exothermic on the triplet surface (−79 kcal/mol) but proceeds stepwise: H^+ dissociates first and then abstracts H to form H_2^+. Pathways for the loss of $CH_2OH_2^{2+}$ include C−O, C−H, and O−H bond dissociation, with higher barriers on the singlet surface (99, 111, and 56 kcal/mol, respectively) than on the triplet surface (27, 34, and 49 kcal/mol, respectively).

Dynamics in a Laser Field. The results of several series of Born−Oppenheimer trajectory calculations for various conditions are listed in Table S5 of the Supporting Information. In the experiments by Yamanouchi and co-workers,[7,8] an initial 40 fs 800 nm pulse ionized methanol to the monocation, and after a delay of 100−800 fs a second pulse ionized the system to a dication. The dication dissociated and the fragments were detected using coincidence momentum imaging. If the ionization by the first pulse is vertical, then neutral CH_3OH is an appropriate starting geometry for the trajectories. If the initial ionization is considered adiabatic, then the optimized monocation geometry is appropriate. Neutral CH_3OH is staggered whereas CH_3OH^+ is eclipsed; both have a rotation barrier of 1 kcal/mol at the CBS-QB3 level of theory. For each set of conditions, we have started half of the monocation trajectories from the staggered CH_3OH geometry and the half from the eclipsed CH_3OH^+ geometry optimized at B3LYP/6-31G(d,p) to cover both ionization scenarios and the nearly free internal rotation.

The classical trajectories were calculated on the ground state Born−Oppenheimer surface with the CAM-B3LYP/6-31G-(d,p) level of theory. The orientations between the laser field and the molecules were chosen randomly. To maximize the interaction of the laser field with the molecule, a trapezoidal pulse was used in the simulations. Trajectories calculated with a

dx.doi.org/10.1021/jp410091b | J. Phys. Chem. A 2014, 118, 1769−1776

Table 1. Fragmentation and Isomerization Percentages[a] for CH_3OH^+

max. field strength (au)	initial kinetic energy (kcal/mol)	$CH_2OH^+ + H$	$HCOH^+ + H_2$	$CH_2OH_2^+$	$CH_3^+ + OH$	$HCO^+ + H + H_2$	no reaction	γ^d	reaction during pulse	reaction after pulse
0.09[b]	75	80.6	9.1	2.8	0.5	0.0	7.1	0.85	42.8	50.1
	100	78.8	13.1	2.3	2.0	1.3	2.5	0.53	58.4	39.0
	125	81.3	10.7	1.3	2.8	3.8	0.0	0.31	66.8	33.2
0.07[b]	75	74.4	9.6	3.5	0.5	0.0	11.9	0.88	29.0	59.1
	100	75.6	13.7	3.8	1.5	1.3	4.1	0.71	46.4	49.5
	125	74.1	15.0	1.0	3.3	5.8	0.8	0.24	62.7	36.5
0.00	75	69.7	12.3	4.6	0.5	0.0	12.8	0.90		
	100	70.7	17.7	5.6	0.0	1.5	4.5	1.00		
	125	71.8	22.1	1.5	1.5	3.1	0.0	0.50		
0.09[c]	125	71.8	16.9	1.0	2.6	7.2	0.5	0.29	58.5	41.0

[a]For trajectories starting from the neutral structure plus trajectories starting from the cation structure. [b]40 fs trapezoid pulse, 800 nm, 400 fs total integration time. [c]40 fs cosine squared pulse, 800 nm, 400 fs total integration time. [d]Fraction of hydrogen migration $\gamma = n(CH_2OH_2^+)/(n(CH_2OH_2^+) + n(CH_3^+ + OH))$.

cosine pulse yielded qualitatively similar results for selected tests. Trajectories were calculated with a field strength of 0.09 and 0.07 au and without a laser field.

An initial test set of 100 trajectories showed that methanol cation picked up a maximum of only 15 kcal/mol from a 40 fs 800 nm pulse with a maximum field strength of 0.09 au. This is not sufficient to overcome even the lowest barriers on the ground state surface of methanol monocation. This suggests that the initial ionization deposits considerable vibrational energy in the cation. Orthant sampling was used to add vibrational kinetic energy to the starting structures. Because the addition of 50 kcal/mol of kinetic energy caused only a few dissociations, most of the trajectories were calculated with 75, 100, and 125 kcal/mol of additional kinetic energy.

Some of the trajectories in which H^+ dissociated during the pulse showed a very large gain in energy from the laser field. A closer examination of these trajectories revealed that at large C−H distances, the charge on the hydrogen varied from H^+ to $H^\bullet$ to H^- as the field changed sign. This is an artifact of calculating the lowest energy state in the Born−Oppenheimer approximation (i.e., not taking into account the electron dynamics). Because the energy gain and charge oscillation was not a problem until the C−H distance became fairly large, these trajectories were terminated at 3 Å and were classified as H dissociations. Those trajectories that did not fragment either showed no change or underwent 1,2 hydrogen migration.

Trajectories for the methanol radical cation were started from both the staggered CH_3OH geometry and the eclipsed CH_3OH^+ geometry with 75, 100, and 125 kcal/mol of initial vibrational kinetic energy in addition to zero point energy. For each case about 200 trajectories were integrated for 400 fs, for a total of ca. 1200 trajectories. The 40 fs trapezoidal laser pulse was oriented randomly and had a maximum field strength of 0.09 au (corresponding to an intensity of 2.9×10^{14} W cm^{-2}). Because the two starting geometries gave similar branching ratios (see Table S5 in the Supporting Information), the data have been combined. The results are reported as percentages in Table 1 and are summarized graphically in Figure 6. For each set of initial conditions, $CH_3OH^+ \rightarrow CH_2OH^+ + H$ was the dominant channel, accounting for about 80% of the trajectories. Loss of H_2 occurred in 9−13% of the trajectories. The $CH_3^+ + OH$ and $CH_2OH_2^+$ products were seen in only 1−3% of the cases. About 7% of the trajectories did not fragment or isomerize in 400 fs with 75 kcal/mol of initial energy, but all trajectories reacted within 400 fs with 125 kcal/mol. An

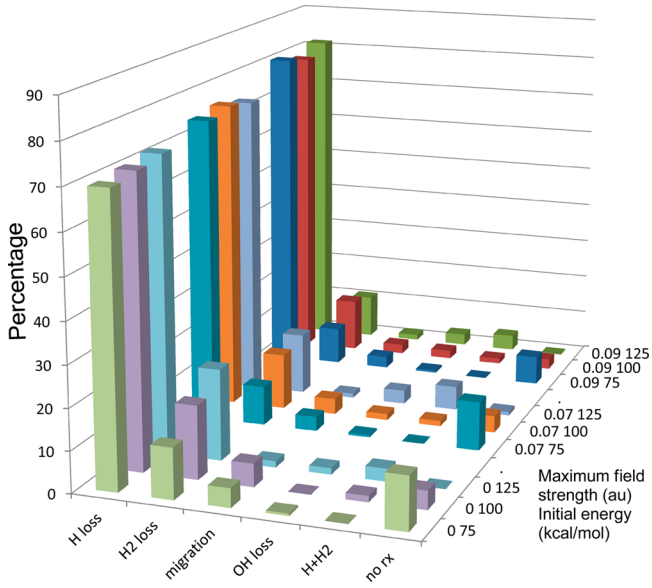

Figure 6. Fragmentation and isomerization percentages for CH_3OH^+ at maximum field strengths of 0, 0.07, and 0.09 au with 75, 100, and 125 kcal/mol initial kinetic energy (see Table 1 for details).

examination of the initial orientations of the molecule in electric field of the laser did not reveal a discernible directional preference for any of the reaction channels. Analysis of the products of $CH_3OH^+ \rightarrow CH_2OH^+ + H$ trajectories did show a higher probability for hydrogen ejection aligned with the field.

The initial kinetic energy had a noticeable effect on the product ratios. The amount of $CH_3^+ + OH$ increased with increasing energy, as expected for this high energy dissociation channel. The yield of $HCOH^+ + H_2$ stayed about the same but the amount of hydrogen migration to give $CH_2OH_2^+$ decreased as the initial kinetic energy was raised. Although the yields of $CH_2OH_2^+$ and $CH_3^+ + OH$ were relatively small, the fraction of hydrogen migration $\gamma = n_{mig}/(n_{mig} + n_{OH})$ decreased significantly as the initial energy was increased.

The amount of initial energy also affected the reaction times. With 75 kcal/mol initial energy, 43% of the trajectories reacted within the 40 fs pulse. This rose to 67% with an initial energy of 125 kcal/mol. The reactions within the pulse were primarily $CH_3OH^+ \rightarrow CH_2OH^+ + H$. Only about 20−40% of the hydrogen migrations and $H_2 + HCOH^+$ reaction occurred within the pulse.

dx.doi.org/10.1021/jp410091b | J. Phys. Chem. A 2014, 118, 1769−1776

The effect of the laser pulse intensity can also be compared in Table 1. When the maximum field strength was reduced from 0.09 to 0.07 au, the percentage of $CH_2OH^+ + H$ decreased and the number of unreactive trajectories increased. The percentage of trajectories that dissociate within the pulse also decreased. The cosine squared pulse with a maximum field strength of 0.09 au yields results comparable to the 0.07 au trapezoidal pulse. When the maximum field strength was reduced to zero and CH_3OH^+ had only the added kinetic energy, $CH_3OH^+ \rightarrow CH_2OH^+ + H$ was still the dominant channel. The number of unreactive trajectories increased somewhat, but the percentages for H loss, H migration, and H_2 loss were about the same as for the 0.07 au pulse. However, there was little OH loss.

In the experimental time-of-flight mass spectrum of CH_3OH ionized by an intense 60 fs 800 nm laser pulse, the CH_2OH^+/CH_3O^+ peak is almost twice the size of the parent peak.[2] This is in keeping with the large number of $CH_3OH^+ \rightarrow CH_2OH^+ + H^+$ dissociations seen in the trajectory calculations (80% for a maximum field strength of 0.09 au). The $HCOH^+ + H_2$ dissociations are the next most abundant trajectories (9–13%). The experimental mass spectrum shows a $HCOH^+/CH_2O^+$ peak that is about 1/10th the size of CH_2OH^+/CH_3O^+. The HCO^+/COH^+ peak is the third largest in the experimental spectrum and can come from loss of H_3^+ or secondary fragmentation of CH_2OH^+ or $HCOH^+$ (calculated barriers of 82 and 33 kcal/mol[15]). The trajectory calculations show that HCO^+ arises from H dissociation followed by H_2 loss, and from H_2 loss followed by H dissociation. The amount of HCO^+ increases from 0 to 4% as the energy increases from 75 to 125 kcal/mol. Up to 3% of the trajectories produce $CH_3^+ + OH$, in accord with the small CH_3^+ peak seen in the spectrum. The CH_3OH^+ trajectories did not yield any H^+, H_3^+, OH^+, CH^+, or CH_2^+. In the experimental mass spectrum, these fragments are probably produced from doubly or triply ionized methanol[1−4] or from subsequent ionization of neutral fragments from the dissociation of the monocation.

Analysis of the mass spectrum peak for H_2^+ ejected from methanol dication indicates a kinetic energy release (KER) of 4.3 eV.[1] The present calculations are used to estimate the maximum KER as the energy difference between the barrier to dissociation and the dissociated product, or between vertically ionized CH_3OH^{2+} and the products (whichever is larger). The calculated KER for H_2^+ from the triplet methanol dication is 4.5 eV. The singlet methanol dication relaxes to $H_2–HCOH^{2+}$ (Figure 5) and can readily lose H_2^+, yielding an estimated KER of 4.1 eV. Coincidence momentum imaging gives ∼5.7 eV for the kinetic energy of $CH_3^+ + OH^+$ and $CH_2^+ + H_2O^+$ from the methanol dication in pump–probe experiments.[6−8] The estimated KER for these two channels on the triplet surface (5.6 and 5.2 eV, respectively) is in better agreement with experiment than the KER calculated from the singlet surface (4.5 and 4.2 eV).

In the pump–probe studies, both migration and dissociation are seen for the methanol cation. The Born–Oppenheimer trajectory calculations on the ground state surface show that the methanol cation gains less than 15 kcal/mol from a 40 fs trapezoid 800 nm pulse with a maximum field strength of 0.09 au. This is not enough to overcome the barriers for hydrogen migration or fragmentation. Therefore, a considerable amount of energy must be deposited in the cation during the ionization process by the pump pulse. Because the 800 nm pulse is in the optical range, this could lead to electronic excitation of the cation. If nonradiative decay is fast, the electronic excitation energy would be converted to vibrational energy in the ground state cation, which then has enough energy to overcome the reaction barriers. This process is modeled in the present, initial study by calculating Born–Oppenheimer trajectories on the ground state surface with added vibrational kinetic energy. Alternatively, isomerization and fragmentation may occur on one or more excited states of the cation or could be the result of coupled nuclear-electron dynamics during the pulse. These scenarios can be addressed in future studies.

Experimental studies comparing the $CH_2OH_2^+$ and $CH_3^+ + OH$ channels find that the fraction of hydrogen migration $\gamma = \eta_{mig}/(\eta_{mig} + \eta_{OH})$ changes only a little, from 0.24 to 0.20, as the laser power is increased by a factor of ten.[8] For the trajectory calculations, this ratio decreases from about 0.8 to 0.3 as the added vibrational energy is increased from 75 to 125 kcal/mol. This suggests that more than 125 kcal/mol of vibrational energy may be deposited in methanol cation by the ionization process. The experimental kinetic energy plots show two distinct regions, above and below 3.8 eV.[7] (a) For energies above 3.8 eV, γ does not depend on the delay time between the pump and probe pulses. This is attributed to ionization of $CH_2OH_2^+$ and CH_3OH^+ near their equilibrium geometry by the probe laser pulse. The trajectory calculations show that isomerization to $CH_2OH_2^+$ does occur sufficiently rapidly on the ground state surface of the monocation if enough vibrational energy is added to overcome the barrier for the migration; the nonreactive trajectories yield CH_3OH^+ near its equilibrium geometry. (b) Below 3.8 eV the kinetic energy release decreases as a function of the delay time between the pump and probe laser pulses. This has been interpreted as the gradual lengthening of the C–O bond in $CH_2OH_2^+$ and CH_3OH^+ toward dissociation before being ionized by the probe pulse. With 100–125 kcal/mol of added vibrational energy, an appreciable amount of C–O dissociation is seen for CH_3OH^+. However, very little C–O dissociation is seen for $CH_2OH_2^+$. One possibility is that more vibrational kinetic energy must be added to obtain enough $CH_2OH_2^+$ dissociation. More likely, the lack of $CH_2OH_2^+ \rightarrow CH_2^+ + H_2O$ trajectories on the ground state potential energy surface may indicate that the observed decrease in the kinetic energy release as a function of delay time seen below 3.8 eV may be due to dissociation on excited state surfaces or coupled nuclear-electron dynamics during the pump pulse.

SUMMARY

The potential energy surfaces for the isomerization and fragmentation of CH_3OH, CH_3OH^+, and singlet and triplet CH_3OH^{2+} were explored using the B3LYP, CAM-B3LYP, CBS-QB3, and CBS-APNO levels of theory. In agreement with previous studies, $CH_2OH_2^+$ and $CH_2OH_2^{2+}$ were found to be more stable than CH_3OH^{n+}. Barriers for $CH_3OH^+ \rightarrow CH_2OH_2^+$ isomerization were computed to be within a few kcal/mol of the barriers for H and H_2 loss. The calculated potential energies yielded estimates of kinetic energy releases for various product channels that were in good accord with experimental observations. Classical trajectory calculations were carried out with the CAM-B3LYP/6-31G(d,p) level of theory for methanol monocation on the ground state potential energy surface in the presence of the laser field (40 fs 800 nm pulse with an intensity of 2.9×10^{14} W/cm^2, equivalent to a field strength of 0.09 au). The simulations showed that unactivated CH_3OH^+ did not gain enough energy to dissociate. When 75–125 kcal/mol of vibrational energy was added to the starting

structures to simulate extra energy deposited by the ionization, most of the trajectories resulted in fragmentation or isomerization. The dominant product was H + CH_2OH^+ (79−81%) with H_2 + $HCOH^+$ next most abundant (9−13%). Isomerization and C−O dissociation of CH_3OH^+ occurred less frequently (1−3% each); C−O dissociation of $CH_2OH_2^+$ occurred in very few trajectories. Experimental results showed that C−O dissociation occurred in a fraction of the CH_3OH^+ and $CH_2OH_2^+$ molecules after the pulse. The fact that very few $CH_2OH_2^+ \rightarrow CH_2^+ + H_2O$ events were seen in the various simulations on the ground state surface (only 3 out of a total of 3200 trajectories) suggests that some of the C−O dissociation processes occur on excited state surfaces or are due to coupled nuclear-electron dynamics during the pump pulse.

■ ASSOCIATED CONTENT

Supporting Information

Tables of relative enthalpies and number of fragmentation and isomerization tranjectories, figure of dipole moment vs field strength. Spreadsheet of the energetic data at various levels of theory. File containing the structures and Cartesian coordinates for selected molecules. This information is available free of charge via the Internet at http://pubs.acs.org

■ AUTHOR INFORMATION

Notes

The authors declare no competing financial interest.

■ ACKNOWLEDGMENTS

This work was supported by a grant from the National Science Foundation (CHE1212281). Wayne State University's computing grid provided computational support.

■ REFERENCES

(1) Furukawa, Y.; Hoshina, K.; Yamanouchi, K.; Nakano, H. Ejection of Triatomic Hydrogen Molecular Ion from Methanol in Intense Laser Fields. *Chem. Phys. Lett.* **2005**, *414*, 117−121.

(2) Okino, T.; Furukawa, Y.; Liu, P.; Ichikawa, T.; Itakura, R.; Hoshina, K.; Yamanouchi, K.; Nakano, H. Coincidence Momentum Imaging of Ejection of Hydrogen Molecular Ions from Methanol in Intense Laser Fields. *Chem. Phys. Lett.* **2006**, *419*, 223−227.

(3) Okino, T.; Furukawa, Y.; Liu, P.; Ichikawa, T.; Itakura, R.; Hoshina, K.; Yamanouchi, K.; Nakano, H. Ejection Dynamics of Hydrogen Molecular Ions from Methanol in Intense Laser Fields. *J. Phys. B* **2006**, *39*, S515−S521.

(4) Liu, P.; Okino, T.; Furukawa, Y.; Ichikawa, T.; Itakura, R.; Hoshina, K.; Yamanouchi, K.; Nakano, H. Three-body Sequential Coulomb Explosions of CH_3OD^{3+} Induced by Intense Laser Fields. *Chem. Phys. Lett.* **2006**, *423*, 187−191.

(5) Okino, T.; Furukawa, Y.; Liu, P.; Ichikawa, T.; Itakura, R.; Hoshina, K.; Yamanouchi, K.; Nakano, H. Coincidence Momentum Imaging of Ultrafast Hydrogen Migration in Methanol and Its Isotopomers in Intense Laser Fields. *Chem. Phys. Lett.* **2006**, *423*, 220−224.

(6) Itakura, R.; Liu, P.; Furukawa, Y.; Okino, T.; Yamanouchi, K.; Nakano, H. Two-body Coulomb Explosion and Hydrogen Migration in Methanol Induced by Intense 7 and 21 fs Laser Pulses. *J. Chem. Phys.* **2007**, *127*, 104306.

(7) Xu, H.; Marceau, C.; Nakai, K.; Okino, T.; Chin, S.-L.; Yamanouchi, K. Communication: Two Stages of Ultrafast Hydrogen Migration in Methanol Driven by Intense Laser Fields. *J. Chem. Phys.* **2010**, *133*, 071103.

(8) Xu, H.; Okino, T.; Kudou, T.; Yamanouchi, K.; Roither, S.; Kitzer, M.; Batuska, A.; Chin, S.-L. Effect of Laser Parameters on Ultrafast Hydrogen Migration in Methanol Studied by Coincidence Momentum Imaging. *J. Phys. Chem. A* **2012**, *116*, 2686−2690.

(9) Harding, L. B.; Schlegel, H. B.; Krishnan, R.; Pople, J. A. Moller-Plesset Study of the H_4CO Potential-Energy Surface. *J. Phys. Chem.* **1980**, *84*, 3394−3401.

(10) Harding, L. B.; Schlegel, H. B.; Krishnan, R.; Pople, J. A. *Theoretical Studies on the Unimolecular Decomposition of Methanol in Potential Energy Surfaces and Dynamics Calculations*; Truhlar, D. G., Ed.; Plenum: New York, 1981; pp 169−183.

(11) Yu, H. G.; Muckerman, J. T. MRCI Calculations of the Lowest Potential Energy Surface for CH_3OH and Direct Ab Initio Dynamics Simulations of the O(D-1)+CH_4 Reaction. *J. Phys. Chem. A* **2004**, *108*, 8615−8623.

(12) Bouma, W. J.; Nobes, R. H.; Radom, L. The Methylenoxonium Radical Cation ($CH_2OH_2^{+\cdot}$) - A Surprisingly Stable Isomer of the Methanol Radical Cation. *J. Am. Chem. Soc.* **1982**, *104*, 2929−2930.

(13) Bouma, W. J.; Macleod, J. K.; Radom, L. Experimental-Evidence for fhe Existence of a Stable Isomer of CH_3OH^+ - the Methylenoxonium Radical Cation, $CH_2OH_2^+$. *J. Am. Chem. Soc.* **1982**, *104*, 2930−2931.

(14) Holmes, J. L.; Lossing, F. P.; Terlouw, J. K.; Burgers, P. C. The Radical Cation $[CH_2OH_2]^{+\cdot}$ and Related Stable Gas-Phase Ion-Dipole Complexes. *J. Am. Chem. Soc.* **1982**, *104*, 2931−2932.

(15) Ma, N. L.; Smith, B. J.; Pople, J. A.; Radom, L. Rearrangement and Dissociative Reactions of the Methanol Radical Cation ($CH_3OH^{+\cdot}$) - A Comparison of Theory and Experiment. *J. Am. Chem. Soc.* **1991**, *113*, 7903−7912.

(16) Curtiss, L. A.; Raghavachari, K.; Trucks, G. W.; Pople, J. A. Gaussian-2 Theory for Molecular-Energies of 1st-Row and 2nd-Row Compounds. *J. Chem. Phys.* **1991**, *94*, 7221−7230.

(17) Wiest, O. Density Functional Theory Studies of the Methanol Radical Cation Hypersurface. *J. Mol. Struct. (THEOCHEM)* **1996**, *368*, 39−48.

(18) Ma, N. L.; Smith, B. J.; Radom, L. Refined Thermochemistry for the Methanol Radical Cation ($CH_3OH^{+\cdot}$) and Its Distonic Isomer ($CH_2OH_2^{\cdot+}$). *J. Phys. Chem.* **1992**, *96*, 5804−5807.

(19) Gauld, J. W.; Glukhovtsev, M. N.; Radom, L. The Structure of the Methanol Radical Cation: An Artificially Short C-O Bond with MP2 Theory. *Chem. Phys. Lett.* **1996**, *262*, 187−193.

(20) Ruhl, E.; Price, S. D.; Leach, S.; Eland, J. H. D. Charge Separation Mass-Spectrometry 2. Methyl Compounds. *Int. J. Mass Spectrom.* **1990**, *97*, 175−201.

(21) Eland, J. H. D.; Trevesbrown, B. J. The Fragmentation of Doubly Charged Methanol. *Int. J. Mass Spectrom.* **1992**, *113*, 167−176.

(22) Bouma, W. J.; Radom, L. Methyleneoxonium and Hydroxymethylene Dications - Dicationic Analogs of Ethylene and Acetylene. *J. Am. Chem. Soc.* **1983**, *105*, 5484−5486.

(23) Yates, B. F.; Bouma, W. J.; Radom, L. Ylide Dications - an Examination of 1st-Row and 2nd-Row Systems. *J. Am. Chem. Soc.* **1986**, *108*, 6545−6554.

(24) Li, X. S.; Schlegel, H. B. Ab Initio Classical Trajectory Calculations of Acetylene Dication Dissociation. *J. Phys. Chem. A* **2004**, *108*, 468−472.

(25) Psciuk, B. T.; Tao, P.; Schlegel, H. B. Ab Initio Classical Trajectory Study of the Fragmentation of C3H4 Dications on the Singlet and Triplet Surfaces. *J. Phys. Chem. A* **2010**, *114*, 7653−7660.

(26) Zhou, J.; Schlegel, H. B. Dissociation of H_2NCH Dication in a Strong Laser Field. *J. Phys. Chem. A* **2011**, *115*, 8375−8379.

(27) Lee, S. K.; Li, W.; Schlegel, H. B. HCO+ Dissociation in a Strong Laser Field: An Ab Initio Classical Trajectory Study. *Chem. Phys. Lett.* **2012**, *536*, 14−18.

(28) Lee, S. K.; Suits, A. G.; Schlegel, H. B.; Li, W. A Reaction Accelerator: Mid-infrared Strong Field Dissociation Yields Mode-Selective Chemistry. *J. Phys. Chem. Lett.* **2012**, *3*, 2541−2547.

(29) Frisch, M. J.; Trucks, G. W.; Schlegel, H. B.; Scuseria, G. E.; Robb, M. A.; et al. *Gaussian Development Version*; Revision H.20; Gaussian, Inc.: Wallingford, CT, 2010.

(30) Ochterski, J. W.; Petersson, G. A.; Montgomery, J. A. A Complete Basis Set Model Chemistry. 5. Extensions to Six or More Heavy Atoms. *J. Chem. Phys.* **1996**, *104*, 2598−2619.
(31) Montgomery, J. A.; Frisch, M. J.; Ochterski, J. W.; Petersson, G. A. A complete basis set model chemistry. VI. Use of density functional geometries and frequencies. *J. Chem. Phys.* **1999**, *110*, 2822−2827.
(32) Curtiss, L. A.; Redfern, P. C.; Raghavachari, K. Gaussian-4 Theory. *J. Chem. Phys.* **2007**, *126*, 084108.
(33) Vosko, S. H.; Wilk, L.; Nusair, M. Accurate Spin-Dependent Electron Liquid Correlation Energies for Local Spin-Density Calculations - A Critical Analysis. *Can. J. Phys.* **1980**, *58*, 1200−1211.
(34) Becke, A. D. Density-Functional Exchange-Energy Approximation with Correct Asymptotic Behavior. *Phys. Rev. A* **1988**, *38*, 3098−3100.
(35) Lee, C. T.; Yang, W. T.; Parr, R. G. Development of the Colle-Salvetti Correlation-Energy Formula into a Functional of the Electron Density. *Phys. Rev. B* **1988**, *37*, 785−789.
(36) Becke, A. D. Density-Functional Thermochemistry. 3. The Role of Exact Exchange. *J. Chem. Phys.* **1993**, *98*, 5648−5652.
(37) Stephens, P. J.; Devlin, F. J.; Chabalowski, C. F.; Frisch, M. J. Ab-Initio Calculations of Vibrational Absorption and Circular-Dichroism Spectra Using Density-Functional Force-Fields. *J. Phys. Chem.* **1994**, *98*, 11623−11627.
(38) Yanai, T.; Tew, D. P.; Handy, N. C. A New Hybrid Exchange-Correlation Functional Using the Coulomb-Attenuating Method (CAM-B3LYP). *Chem. Phys. Lett.* **2004**, *393*, 51−57.
(39) Schlegel, H. B. Molecular Dynamics in Strong Laser Fields: A New Algorithm for Ab Initio Classical Trajectories. *J. Chem. Theory Comput.* **2013**, *9*, 3293−3298.
(40) Bakken, V.; Millam, J. M.; Schlegel, H. B. Ab Initio Classical Trajectories on the Born-Oppenheimer Surface: Updating Methods for Hessian-Based Integrators. *J. Chem. Phys.* **1999**, *111*, 8773−8777.
(41) Wu, H.; Rahman, M.; Wang, J.; Louderaj, U.; Hase, W. L.; Zhuang, Y. Higher-Accuracy Schemes for Approximating the Hessian from Electronic Structure Calculations in Chemical Dynamics Simulations. *J. Chem. Phys.* **2010**, *133*, 074101.
(42) Bunker, D. L.; Hase, W. L. Non-RRKM Unimolecular Kinetics - Molecules in General, and CH3NC in Particular. *J. Chem. Phys.* **1973**, *59*, 4621−4632.
(43) Sosa, C.; Schlegel, H. B. Carbene and Silylene Insertion Reactions - Ab Initio Calculations on the Effects of Fluorine Substitution. *J. Am. Chem. Soc.* **1984**, *106*, 5847−5852.